

The Effect of Series and Shunt Redundancy on Power Semiconductor Reliability

Mohsen Hasan Babayi Nozadian[†], Mohammad Shadnam Zarbil^{*}, and Mehdi Abapour^{*}

^{†,*}Department of Electrical and Computer Engineering, University of Tabriz, Tabriz, Iran

Abstract

In different industrial and mission oriented applications, redundant or standby semiconductor systems can be implemented to improve the reliability of power electronics equipment. The proper structure for implementation can be one of the redundant or standby structures for series or parallel switches. This selection is determined according to the type and failure rate of the fault. In this paper, the reliability and the mean time to failure (MTTF) for each of the series and parallel configurations in two redundant and standby structures of semiconductor switches have been studied based on different failure rates. The Markov model is used for reliability and MTTF equation acquisitions. According to the different values for the reliability of the series and parallel structures during SC and OC faults, a comprehensive comparison between each of the series and parallel structures for different failure rates will be made. According to the type of fault and the structure of the switches, the reliability of the switches in the redundant structure is higher than that in the other structures. Furthermore, the performance of the proposed series and parallel structures of switches during SC and OC faults, results in an improvement in the reliability of the boost dc/dc converter. These studies aid in choosing a configuration to improve the reliability of power electronics equipment depending on the specifications of the implemented devices.

Key words: Failure rate, Markov model, Mean time to failure, Redundant system, Reliability

NOMENCLATURE

λ_{1N-sh} :	Failure rate of switch 1 when switch 2 is operating.	sh :	SC fault occurrence on a switch.
λ_{1F-sh} :	SC failure rate of switch 1 when only switch 1 is operating.	o :	OC fault occurrence on a switch.
λ_{1N-o} :	OC failure rate of switch 1 when switch 2 is operating.	s :	Standby structure of a switch.
λ_{1F-o} :	OC failure rate of switch 1 when only switch 1 is operating.	$S.C Sys$:	System short-circuit.
λ_{2N-sh} :	SC failure rate of switch 2 when switch 1 is operating.	$O.C Sys$:	System open-circuit.
λ_{2F-sh} :	SC failure rate of switch 2 when only switch 2 is operating.	λ_b :	Base failure rate.
λ_{2N-o} :	OC failure rate of switch 2 when switch 1 is operating.	π_T :	Temperature factor.
λ_{2F-o} :	OC failure rate of switch 2 when only switch 2 is operating.	π_E :	Environmental factor.
P_s :	Perfect operation relay probability.	π_Q :	Quality factor.
n :	Normal switching operation.		

I. INTRODUCTION

Although the technology of semiconductor power devices has been improved, they are still known as the weakest devices in power system technology [1]. The most commonly occurring failure mechanisms are thermal runaway, bursting and reverse voltage. Most power electronics systems are not equipped with redundant systems, which means that any fault occurrences in devices or sub-systems result in a failure [2]. These unscheduled interruptions, cause security concerns and reduce the advantages of power electronics systems. That is

Manuscript received Nov. 20, 2015; accepted Apr. 4, 2016

Recommended for publication by Associate Editor Hao Ma.

[†]Corresponding Author: m.hasanbabayi@tabrizu.ac.ir

Tel: +98-411-3393704, Fax: +98-411-3300829, Tabriz University

^{*}Department of Electrical and Computer Engineering, University of Tabriz, Iran

why recent papers have focused on the reliability of power electronics systems. Many methods have been presented in the literature for improvements in the reliability of power electronics systems, such as active supervising, fault management, and establishing fault resistibility using control strategies and restructuring [3]-[7]. The reliability prediction and modeling of high power switches (IGBTs and MOSFETs) have been studied in [8]-[12]. Reference [13] conducts a brief analysis of an assessment of reliability and the development of power electronics in three levels: 1) indexes and methods for the reliability assessment of current systems; 2) reliability improvement of available systems using algorithmic solutions with no hardware change; and 3) designing solutions according to reliability that are based on resistant functioning in fault conditions. In reference [14] a review of the improvement in the reliability of capacitors for the DC-links in power electronic converters is presented. One of the main methods to establish fault resistibility and to reduce unexpected system failures is to design using redundant or standby elements which is introduced in [15]-[17]. Different studies on multi-level inverters have been done that include the effects of redundant parts, different frameworks, control strategies and fault control. The reliability of multi-level inverters is calculated and presented in [18]. In this article, the reliability of two, three and five level inverters is calculated and compared with each other. Given that the reliability of power electronics inverters depends on the accurate operation of power electronics switches, the proper switching function is an important issue in terms of the reliability of power electronics devices. Accordingly, in [19] the reliability of MOSFET switches in parallel and standby structures and with different numbers of redundant elements is discussed, and the effect of power losses on junction thermal increases and its effect on the failure rate of MOSFET switches is analyzed. In this paper, the Markov model is used to determine the reliability and the Mean Time To Failure (MTTF). In mission-oriented systems, reliability is directly proportional to the MTTF. Therefore, by increasing the operation time, the reliability will be improved. Since the impairment of power switches can be SC or OC, it is necessary to study the switching functions in series and in parallel separately, and to choose the best configuration to improve the switching reliability. In [20] mathematical models have been presented to quantitatively evaluate the reliability of parallel inverters, and a framework has been proposed to determine the number of inverters in parallel in terms of reliability and cost optimization. A new approach for the mitigation of permanent-magnet ac motors and a methodology to calculate the mean time between failures both with and without mitigation have been presented in [21]. In reference [22] an analysis of a high-power and high frequency voltage-fed inverter with a series resonant load circuit has been presented, and it is characterized by a

full-bridge inverter composed of isolated-gate bipolar transistors. [23] calculates the reliability of an interleaved boost DC-DC converter, and presents a comparison between this and the reliability of the conventional boost converter.

This article discusses the reliability and MTTF for two series and parallel configurations without the repair ability in three structures: a “redundant structure equipped with similar relays”, a “standby redundant structure with a relay” and a “redundant structure without a relay.” In addition, the failure rate of the power switches has been studied in both short-circuit and open-circuit fault conditions.

II. THE UTILIZATION OF REDUNDANT SWITCHES FOR RELIABILITY ENHANCEMENT

The ability of a system to perform its duty under circumferential conditions and specified exploitations for a certain period of time is called the reliability of the system. There are two analytic and simulation methods for reliability evaluation and MTTF calculation, and the analytic method is used in this paper. There are different ways of achieving the reliability enhancement of a system such as: implementation of high-quality utilities, using redundant equipment, variation in products, providing spare parts and repair-observance. The main method for improving reliability is the usage of redundant equipment. In this paper, a redundant switch connection has been proposed to increase the MTTF and consequently the reliability. In addition, different structures have been compared. Redundant switches can be added to the system in both series and parallel configurations. In this article, [3] structures are considered both in parallel and in series connections of redundant switches: redundant with relays in similar structures, standby redundant with relay and redundant without relay. These structures are described in the upcoming sections. Before any analysis, it has to be mentioned that these relays only operate during fault conditions of power electronics switches. In other words, they do the task of removing the faulty part or entering the safe part just once. In a specific alternation period and frequency, they are not switched on/off. Therefore, it is not necessary to use switches with fast-switching capability. According to the fact that the control system and the power circuit are two separate parts, redundant and standby systems are discussed and their reliabilities are compared with each other in this paper. It is assumed that switches are controlled ideally i.e. there is no problem in controlling the power switch gates. It is possible to discuss the control contribution for each of the switches using the Markov model.

A. Series Configuration

In series circuits, an OC fault condition in one part of the system results in a failure of the whole system. Meanwhile, in a SC fault condition in the same circuit, the system can keep on operating. Therefore, it is enough to have only one active

part in the system to provide a routine system process during a SC fault condition. According to the above mentioned conditions, relays are used in series circuits so that during an OC fault condition, they can remove the damaged (faulty) part from circuit to guarantee the routine procedures of the system. In this paper, a series configuration with two forming parts (power electronics switches) has been analyzed. The challenge here is to choose the best initial structure for the relays in the two-part series configuration, so that the system can have a better structure. Therefore, an analysis had been done on the 3 structures of the relays i.e. “both are initially open”, “one open- one closed” and “no relays.” Finally, by finding the Markov model of these structures, it is possible to acquire the $R(t)$ and MTTF equations. By comparing these equations, the best structure for a two-part series configuration can be found.

1) Markov Modeling and Reliability & MTTF Calculations of a Redundant Structure with Similar Relays (both Relays are Initially Open)

In this structure, two switches are connected together in series, and both of these switches are also in parallel with a relay. Both of the relays are initially open and during an OC fault occurrence for one of the switches, its respective relay is closed to remove the faulty switch from the circuit. During a SC fault condition in a switch, the system can perform regularly without the need to close the relay. In this configuration, half of the total network voltage will be seen on each of the switches. Therefore, the failure rate of the switches will be lower in this structure. However, when one switch is damaged, the grid voltage completely goes through the second switch and the failure rate of the second switch is high. Fig. 1 shows the series configuration with two open relays.

Fig. 2 shows the state space or the Markov model for the series configuration with two open relays. As shown in Fig. 2, nine different states are possible in this configuration. Consider that both parts of the system initially work in a normal state and that both of the relays are initially open. If a SC fault occurs in switch 1, state 1 changes to state 2 with a failure rate of λ_{1N-sh} in this state. Under the same fault condition for switch 2, a transition from state 1 to state 3 occurs with a failure rate of λ_{2N-sh} . No interference of the relaying probability (P_s) is necessary, because there is no need for relay operation in these states. Consider state 1 when an OC fault occurs in one of the switches. If the relay operates correctly with a failure rate of $P_s \lambda_{1N-o}$ or $P_s \lambda_{2N-o}$, the transition is from states 5 or 6, respectively. Otherwise it will get to state 7 with a failure rate of $(1-P_s) \lambda_{1N-o}$ or $(1-P_s) \lambda_{2N-o}$ and the system is completely open-circuit.

Because of the large number of parameters and for a better

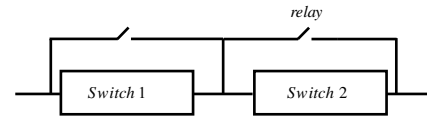


Fig. 1. A series configuration with 2 open relays.

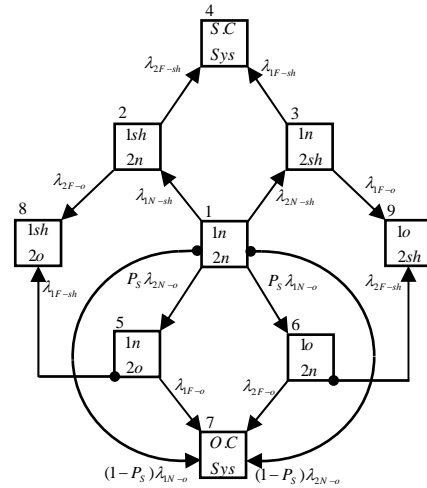


Fig. 2. The Markov model for a series configuration with 2 open relays.

understanding of the MTTF equation, in the final equation of each configuration, some assumptions are made for the sake of an easy comparison:

$$\begin{cases} \lambda_{1N-sh} = \lambda_{2N-sh} = \lambda_{N-sh} \\ \lambda_{1F-sh} = \lambda_{2F-sh} = \lambda_{F-sh} \\ \lambda_{1N-o} = \lambda_{2N-o} = \lambda_{N-o} \\ \lambda_{1F-o} = \lambda_{2F-o} = \lambda_{F-o} \end{cases} \quad (1)$$

According to the Markov model, the probability matrix in this model is named P_{s1} as in the following:

$$P_{s1} = \begin{bmatrix} a_0 & a_1 & a_2 & 0 & a_3 & a_4 & a_5 & 0 & 0 \\ 0 & a_6 & 0 & a_7 & 0 & 0 & 0 & a_8 & 0 \\ 0 & 0 & a_9 & a_{10} & 0 & 0 & 0 & 0 & a_{11} \\ 0 & 0 & 0 & 1 & 0 & 0 & 0 & 0 & 0 \\ 0 & 0 & 0 & 0 & a_9 & 0 & a_{11} & a_{10} & 0 \\ 0 & 0 & 0 & 0 & 0 & a_6 & a_8 & 0 & a_7 \\ 0 & 0 & 0 & 0 & 0 & 0 & 1 & 0 & 0 \\ 0 & 0 & 0 & 0 & 0 & 0 & 0 & 1 & 0 \\ 0 & 0 & 0 & 0 & 0 & 0 & 0 & 0 & 1 \end{bmatrix} \quad (2)$$

The quantities of a_i ($i = 0$ to 11) are given in (2) in the appendix.

The MTTFs of the above mentioned configurations determine the expected lifetime of these configurations. Thus, they can be good measures to compare the reliabilities of the different configurations. To calculate the MTTF, the absorbing state method is used in this paper. When the absorbing state occurs, the state escaping ability of the system is unavailable. However, when starting one non-absorbing state, a new mission starts. Such states are mentioned as

disastrous failures for mission-oriented systems, and their occurrence probability should be the lowest available in order to provide a more reliable operation for the system. Considering P as a stochastic transitional probability matrix, the Q -matrix is formed based on P and by omitting rows and columns of the absorbing state. According to the state space block diagrams in this model, the states 1, 2, 3, 5 and 6 are non-absorbing states that keep the system active. Therefore, the Q -matrix is as follows:

$$Q_{s1} = \begin{bmatrix} a_0 & a_1 & a_2 & a_3 & a_4 \\ 0 & a_6 & 0 & 0 & 0 \\ 0 & 0 & a_9 & 0 & 0 \\ 0 & 0 & 0 & a_9 & 0 \\ 0 & 0 & 0 & 0 & a_6 \end{bmatrix} \quad (3)$$

According to the non-absorbing state method, the MTTF is described by the following equation:

$$MTTF = [I - Q]^{-1} \quad (4)$$

Where I is the Unit Matrix, and placing (2) into the above equation yields:

$$MTTF = \begin{pmatrix} \begin{bmatrix} 1 & 0 & 0 & 0 & 0 \\ 0 & 1 & 0 & 0 & 0 \\ 0 & 0 & 1 & 0 & 0 \\ 0 & 0 & 0 & 1 & 0 \\ 0 & 0 & 0 & 0 & 1 \end{bmatrix} & \begin{bmatrix} a_0 & a_1 & a_2 & a_3 & a_4 \\ 0 & a_6 & 0 & 0 & 0 \\ 0 & 0 & a_9 & 0 & 0 \\ 0 & 0 & 0 & a_9 & 0 \\ 0 & 0 & 0 & 0 & a_6 \end{bmatrix} \end{pmatrix}^{-1} \quad (5)$$

By simplifying (5) and according to the given quantities for a_i ($i = 0$ to 11) in the appendix, starting from state 1, the MTTF can be written as:

$$MTTF_{s1} = \frac{2\lambda_{N-sh} + \lambda_{F-sh} + 2P_S\lambda_{N-o} + \lambda_{F-o}}{2(\lambda_{F-sh} + \lambda_{F-o})(\lambda_{N-sh} + \lambda_{N-o})} \quad (6)$$

In general, the time-dependent probability equation is as follows:

$$\frac{d}{dt} \begin{bmatrix} P_1 \\ P_2 \\ \vdots \\ P_n \end{bmatrix}_{(n \times 1)} = A_{(n \times n)} P(t)_{(n \times n)} \quad (7)$$

$$= \begin{bmatrix} A_{11} & \cdots & A_{1n} \\ \vdots & \ddots & \vdots \\ A_{n1} & \cdots & A_{nn} \end{bmatrix}_{(n \times n)} \times \begin{bmatrix} P_1 \\ P_2 \\ \vdots \\ P_n \end{bmatrix}_{(n \times 1)}$$

According to the probability matrix, the $A_{n \times n}$ matrix is obtained as follows:

$$A_{n \times n} = (P - I)_{n \times n}^T \quad (8)$$

It is assumed that the initial state starting from state 1 is as follows:

$$P(0) = [1 \ 0 \ 0 \ 0 \ 0 \ 0 \ 0 \ 0 \ 0] \quad (9)$$

According to equations (1), (2), (8) and (9), the reliability

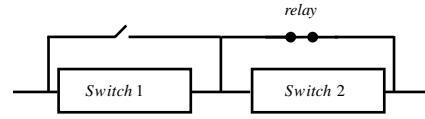


Fig. 3. A series configuration with one open relay and one closed.

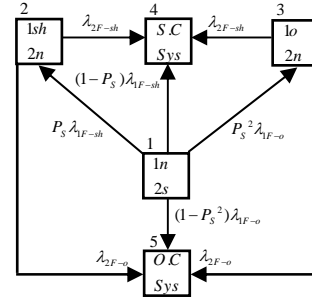


Fig. 4. The Markov model of a series configuration with one open relay and one closed.

is achieved as follows:

$$R_{s1}(t) = e^{-2(\lambda_{N-sh} + \lambda_{N-o})t} + \frac{2(P_S\lambda_{N-o} + \lambda_{N-sh})(e^{-(\lambda_{F-sh} + \lambda_{F-o})t} - e^{-2(\lambda_{N-sh} + \lambda_{N-o})t})}{2(\lambda_{N-sh} + \lambda_{N-o}) - (\lambda_{F-sh} + \lambda_{F-o})} \quad (10)$$

2) Markov Modeling and Reliability & MTTF Calculations of a Standby Redundant Structure with Relays (Initially Relay 1 Open and Relay 2 Closed)

The difference between this structure and the previous one is that here, instead of both relays being initially open, the respective relay for switch 1 is initially open and the corresponding relay of switch 2 is closed. In the case of an OC fault in switch 1, its related relay will be closed to remove the faulty switch from the circuit. At the same time, relay 2 is open to let switch 2 into the circuit, but in the case of a SC fault in switch 1. There is no need for the closure of relay 1 under these conditions and only relay 2 is open. In this configuration, one of the switches is always in operation. Therefore, the whole network voltage is seen in one switch and its failure rate is high. Fig. 3 shows the series configuration with one open and one closed relay.

Fig. 4 presents a Markov model for a series configuration with one open and one closed relay. As shown in Fig. 4, five states are likely to happen in this configuration. Assuming switch 1 is initially working and that the other one is in the standby state, relay 1 is open and the other one is closed. According to the Markov model, the state matrix in this model is named P_{s2} , and is shown as:

$$P_{s2} = \begin{bmatrix} b_0 & b_1 & b_2 & b_3 & b_4 \\ 0 & b_5 & 0 & b_6 & b_7 \\ 0 & 0 & b_5 & b_6 & b_7 \\ 0 & 0 & 0 & 1 & 0 \\ 0 & 0 & 0 & 0 & 1 \end{bmatrix} \quad (11)$$

The quantities of b_i ($i = 0$ to 7) are given in (11) in the appendix. According to the state space block diagram of this model, states 1, 2 and 3 are non-absorbing states that keep the system active. The calculation of the MTTF, is similar to the procedure for the configuration shown in figure 1. According to equation (11), it is obtained as follows:

$$MTTF_{s_2} = \frac{(\lambda_{F-sh} + \lambda_{F-o}) + P_S \lambda_{F-sh} + P_S^2 \lambda_{F-o}}{(\lambda_{F-sh} + \lambda_{F-o})^2} \quad (12)$$

To calculate the reliability, it is assumed that the initial state starts from state 1, and according to equations (1), (8), (9) and (11) the reliability is achieved as follows:

$$R_{s_2}(t) = (1 + P_S \lambda_{F-sh} t + P_S^2 \lambda_{F-o} t) e^{-(\lambda_{F-sh} + \lambda_{F-o})t} \quad (13)$$

3) Markov Modeling and Reliability & MTTF Calculations of a Redundant Structure without a Relay

In this structure, two switches are connected in series without any relay. During an OC fault condition for one of the switches in this configuration, the whole system faces a total failure. However, during a SC fault occurrence in one of the switches, the system can keep on working normally with one switch until the other switch becomes active. In this configuration, half of the network voltage is in each switch. Therefore, the failure rates of the switches are low. During a SC fault condition for one of the switches, the other switch operates normally and supports the total voltage of the network. In this structure, the failure rate of the active switch is higher. On the other hand, during an OC fault condition for one switch, the whole system stops operating. Fig. 5 shows the series configuration without a relay. Fig. 6 presents a Markov model for a series configuration without a relay. As shown in Fig. 6, six states are likely to happen in this configuration. It is assumed that both system parts are initially operating in a normal state.

According to the Markov model, the state matrix in this structure, P_{s_3} is presented as follows:

$$P_{s_3} = \begin{bmatrix} c_0 & c_1 & c_2 & 0 & c_3 \\ 0 & c_4 & 0 & c_5 & c_6 \\ 0 & 0 & c_7 & c_8 & c_9 \\ 0 & 0 & 0 & 1 & 0 \\ 0 & 0 & 0 & 0 & 1 \end{bmatrix} \quad (14)$$

The quantities of c_i ($i = 0$ to 9) have been given in (14) in the appendix. Based on the state space block diagram in this model, states 1, 2 and 3 are non-absorbing states. Therefore, the system will be active. According to equation (14) the MTTF is obtained as follows:

$$MTTF_{s_3} = \frac{2\lambda_{N-sh} + (\lambda_{F-sh} + \lambda_{F-o})}{2(\lambda_{N-sh} + \lambda_{N-o})(\lambda_{F-sh} + \lambda_{F-o})} \quad (15)$$

For calculating the reliability, it is assumed that the initial state starts from state 1, and according to equations (1), (8), (9) and (14) the reliability is achieved as follows:



Fig. 5. A series configuration without a relay.

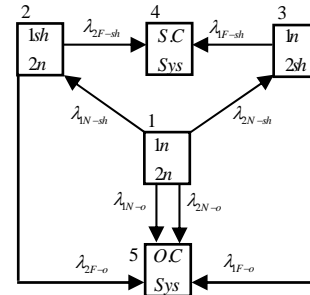


Fig. 6. The Markov model for a series configuration without a relay.

$$R_{s_3}(t) = e^{-2(\lambda_{N-sh} + \lambda_{N-o})t} + \frac{2\lambda_{N-sh} (e^{-(\lambda_{F-sh} + \lambda_{F-o})t} - e^{-2(\lambda_{N-sh} + \lambda_{N-o})t})}{2(\lambda_{N-sh} + \lambda_{N-o}) - (\lambda_{F-sh} + \lambda_{F-o})} \quad (16)$$

B. Parallel Configuration

Unlike series circuits, in parallel circuits during a SC fault in any part of the system, the entire system experiences a failure. In such circuits, during an OC fault condition, the system can continue its regular duty. Therefore, due to the occurrence of an OC fault, the operation of one part leads to the regular operation of the whole system. Under the above conditions in parallel circuits, relays are needed so that during a SC fault condition for one part, the damaged part can be removed from the circuit to guarantee system's routine procedure. Like the previous configuration (series configuration) in this paper, a two-part (switch) parallel configuration has been analyzed. The Markov model of the 3 relaying structures – “both initially closed”, “initially one open and one closed” and “no relay” – and their reliability and MTTF have been calculated.

1) Markov Modeling and Reliability & MTTF Calculations of a Redundant Structure with Similar Relays (both Relays are Initially Closed)

In this configuration, there are two switches in parallel, with each connected to a relay in series. In this structure, both of the relays are initially closed. In the case of a SC fault in one of the switches, its respective relay becomes open to remove the faulty switch from the circuit. However, in an OC fault condition in one of the switches, there is no need for the relay to be open and the system can operate regularly. In this configuration, half of the whole network current goes through each of the switches when both switches are active. Therefore, the failure rate of the switches decreases.

When one of the switches is damaged, the entire current of the network passes through the other switch and its failure

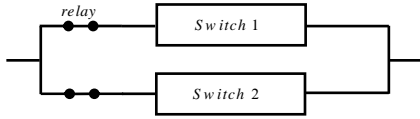


Fig. 7. A parallel configuration with two initially closed relays.

rate increases. Fig. 7 shows the parallel configuration with two initially closed relays. Fig. 8 shows the Markov model of a parallel configuration with two closed relays. As can be seen in Fig. 8, nine possible states can occur in this configuration. It is considered that all of the system parts are initially working in a normal state and that both of the relays are closed. As an example, some probable events in the case of a SC fault in switch 1 are mentioned. Under these conditions with the failure rate of $P_S \lambda_{1N-sh}$, a transition occurs from state 1 to state 2, and with the same fault in switch 2 with the failure rate of $P_S \lambda_{2N-sh}$, the state changes from 1 to 3. Even if none of above states occur, the system gets totally short-circuited. When an OC fault takes place in one of the switches in state 1, because there is no need for relay operation in this state, the relaying probability (P_S) has no effect on the equations. Therefore, the transition to state 5 occurs with the failure rate of λ_{1N-o} .

According to the Markov model, the state matrix for this configuration is shown with P_{p1} as follows:

$$P_{p1} = \begin{bmatrix} d_0 & d_1 & d_2 & d_3 & d_4 & d_5 & 0 & 0 & 0 \\ 0 & d_6 & 0 & d_7 & 0 & 0 & 0 & d_8 & 0 \\ 0 & 0 & d_9 & d_{10} & 0 & 0 & 0 & 0 & d_{11} \\ 0 & 0 & 0 & 1 & 0 & 0 & 0 & 0 & 0 \\ 0 & 0 & 0 & 0 & d_9 & 0 & d_{10} & d_{11} & 0 \\ 0 & 0 & 0 & 0 & 0 & d_6 & d_8 & 0 & d_7 \\ 0 & 0 & 0 & 0 & 0 & 0 & 1 & 0 & 0 \\ 0 & 0 & 0 & 0 & 0 & 0 & 0 & 1 & 0 \\ 0 & 0 & 0 & 0 & 0 & 0 & 0 & 0 & 1 \end{bmatrix} \quad (17)$$

The quantities of d_i ($i = 0$ to 11) have been given in (17) in the appendix. According to the state space block diagram, in this model, states 1, 2, 3, 5 and 6 are non-absorbing states that keep the system active. According to equation (17) the MTTF is obtained as follows:

$$MTTF_{p1} = \frac{2P_S \lambda_{N-sh} + \lambda_{F-sh} + 2\lambda_{N-o} + \lambda_{F-o}}{2(\lambda_{F-sh} + \lambda_{F-o})(\lambda_{N-sh} + \lambda_{N-o})} \quad (18)$$

To calculation the reliability, it is assumed that the initial state starts from state 1, and according to equations (1), (8), (9) and (17) the reliability is obtained as follows:

$$R_{p1}(t) = e^{-2(\lambda_{N-sh} + \lambda_{N-o})t} + \frac{2(\lambda_{N-o} + P_S \lambda_{N-sh})(e^{-(\lambda_{F-sh} + \lambda_{F-o})t} - e^{-2(\lambda_{N-sh} + \lambda_{N-o})t})}{2(\lambda_{N-sh} + \lambda_{N-o}) - (\lambda_{F-sh} + \lambda_{F-o})} \quad (19)$$

2) Markov Modeling and Reliability & MTTF Calculations of Standby Redundant Structure with Relays (Initially Relay 1 Open and Relay 2 Closed)

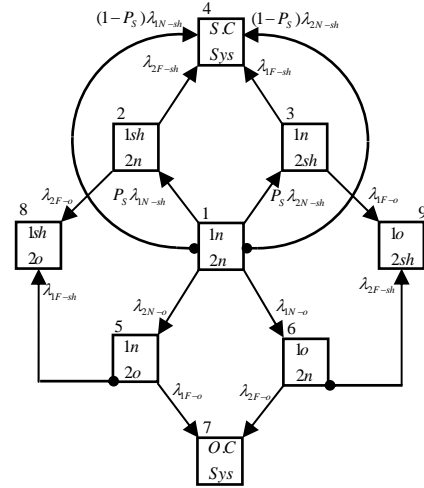


Fig. 8. The Markov model for a parallel configuration with two closed relays.

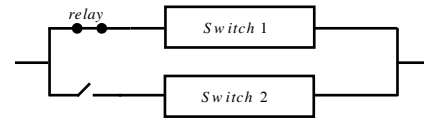


Fig. 9. A parallel configuration with one open and one closed relay.

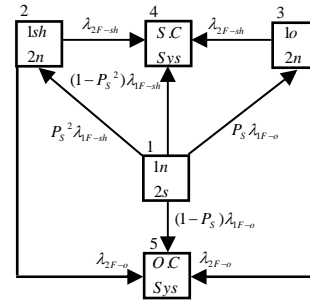


Fig. 10. The Markov Model of a parallel configuration with one open relay and one closed.

In this structure, instead of both relays being initially closed, the corresponding relays for switches 1 and 2 are closed and open, respectively. In the case of a SC fault occurrence in switch 1, its related relay is opened to remove the faulty switch from the circuit. At the same time, relay 2 is closed to bring switch 2 into the circuit. In the case of an OC fault in switch 1, there is no need to open relay 1 and only relay 2 is closed. In this configuration, one of the switches is always active and all of the network current goes through it. In this structure, the failure rate of the operating switch increases. Fig. 9 shows the parallel configuration with one open relay and one closed relay. Fig. 10 shows the Markov model for the parallel configuration with one open relay and one closed relay. As can be seen in Fig. 10, five possible states can occur in this configuration. It is considered that switch 1 is initially active and that the other switch is in the standby state. Therefore, relay 1 is closed and the other relay is open.

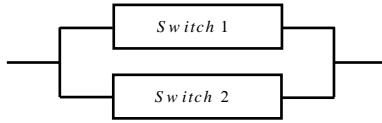


Fig. 11. A parallel configuration without a relay.

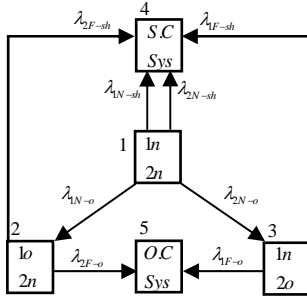


Fig. 12. The Markov Model for a parallel configuration without a relay.

Based on the Markov model, the state matrix in this model, P_{p2} is shown as:

$$P_{p2} = \begin{bmatrix} g_0 & g_1 & g_2 & g_3 & g_4 \\ 0 & g_5 & 0 & g_6 & g_7 \\ 0 & 0 & g_5 & g_6 & g_7 \\ 0 & 0 & 0 & 1 & 0 \\ 0 & 0 & 0 & 0 & 1 \end{bmatrix} \quad (20)$$

The quantity of g_i ($i = 0$ to 7) is given in (20) in the appendix. According to the state space block diagram, the states 1, 2 and 3 are non-absorbing states. Therefore, the system is active. According to equation (20) the MTTF is obtained as follows:

$$MTTF_{p2} = \frac{(\lambda_{F-sh} + \lambda_{F-o}) + P_S^2 \lambda_{F-sh} + P_S \lambda_{F-o}}{(\lambda_{F-sh} + \lambda_{F-o})^2} \quad (21)$$

In order to calculate the reliability, it is assumed that the initial state starts from state 1, and according to equations (1), (8), (9) and (20) the reliability is obtained as follows:

$$R_{s2}(t) = (1 + P_S^2 \lambda_{F-sh} t + P_S \lambda_{F-o} t) e^{-(\lambda_{F-sh} + \lambda_{F-o})t} \quad (22)$$

3) Markov Modeling and Reliability & MTTF Calculations of a Redundant Structure without a Relay

In this structure, two switches are connected in parallel without a relay. In this configuration, in the case of a SC fault in one of the switches, the system experiences a total failure. However, when there is an OC fault condition in one switch, the system can keep on working until the next switch that is not damaged. Half of the network current goes through each switch and the failure rate is low. When one of the switches is under an OC fault condition, the second switch continues working regularly and transfers the entire network current, which results in a higher failure rate. In the case of a SC fault in one switch, the system is totally damaged. Fig. 11 shows

the parallel configuration without a relay. Fig. 12 shows the Markov model for the parallel configuration without a relay. As shown in Fig. 12, five states can occur in this configuration. It is considered that both system parts are initially working in a normal state.

According to the Markov model, the state matrix in this configuration is P_{p3} , and is shown as:

$$P_{p3} = \begin{bmatrix} h_0 & h_1 & h_2 & h_3 & 0 \\ 0 & h_4 & 0 & h_5 & h_6 \\ 0 & 0 & h_7 & h_8 & h_9 \\ 0 & 0 & 0 & 1 & 0 \\ 0 & 0 & 0 & 0 & 1 \end{bmatrix} \quad (23)$$

The quantities of h_i ($i = 0$ to 9) have been given in (23) in the appendix. Based on the state space block diagram, the states 1, 2 and 3 are non-absorbing states. Therefore, the system is active in these states. The MTTF is obtained according to equation (23) as follows:

$$MTTF_{p3} = \frac{2\lambda_{N-o} + (\lambda_{F-sh} + \lambda_{F-o})}{2(\lambda_{N-sh} + \lambda_{N-o})(\lambda_{F-sh} + \lambda_{F-o})} \quad (24)$$

For calculating the reliability, it is assumed that the initial state starts from state 1, and according to equations (1), (8), (9) and (23) the reliability is achieved as follows:

$$R_{p3}(t) = e^{-2(\lambda_{N-sh} + \lambda_{N-o})t} + \frac{2\lambda_{N-o} (e^{-(\lambda_{F-sh} + \lambda_{F-o})t} - e^{-2(\lambda_{N-sh} + \lambda_{N-o})t})}{2(\lambda_{N-sh} + \lambda_{N-o}) - (\lambda_{F-sh} + \lambda_{F-o})} \quad (25)$$

III. THE UTILIZATION OF REDUNDANT SWITCHES FOR RELIABILITY ENHANCEMENT

According to the above analysis, the aim of this study is to find a configuration with the best reliability. Because the current and voltage stresses in switches in parallel operation are less than those in single switch operation, the failure rate is less when two switches work at the same time. These assumptions are independent from the fault type, i.e. they are always true for OC and SC faults. Therefore, it can be written that:

$$\begin{cases} \lambda_{N-sh} \leq \lambda_{F-sh} \\ \lambda_{N-o} \leq \lambda_{F-o} \end{cases} \quad (26)$$

In this article, the SC and the OC failure rates account for 70% and 30% of all failures [24]. The failure rate for each of the power switches is presented in [25]. The MOSFET failure rate has been used in this paper for numerical analysis. The failure rate of power switches depends on environmental conditions, their quality and temperature. It is described as:

$$\lambda = \lambda_b \pi_T \pi_Q \pi_E (f / 10^6 \text{ h}) \quad (27)$$

In the above equation, λ_b is the power switch base failure

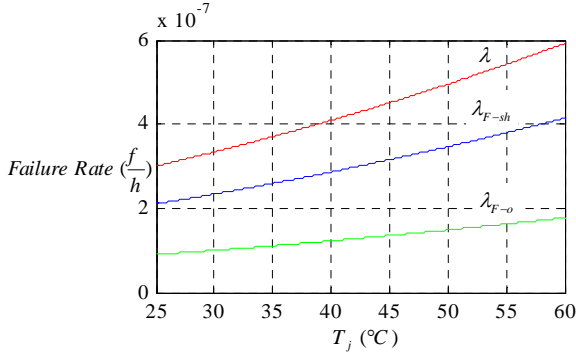


Fig. 13. Changes in the failure rate based on the semiconductor junction temperature.

rate, which is normally related to electric tension and temperature and is equal to $0.06 \times 10^{-6} (f/h)$ for a MOSFET. As the temperature rises, the failure rate increases, and the probability of failure rises. Moreover, the temperature factor π_T is a function of the device junction temperature T_j .

The failure rate also depends on the application of the device in a circuit. The quality and the type of materials used in the fabrication of the device affects its failure rate. More information about the quality factor can be found in MIL-S-19500. In this work, π_Q is considered to be equal to 5. The environment of operation also effects the failure rate of a device. For instance, a device operating on the ground will have a different π_E than a device operating in space. In this paper, the environment for all of the parts is assumed to be the ground (G_B). Therefore, $\pi_E = 1$ is considered in the reliability and MTTF calculations.

According to (27) and the above cases, the failure rate of a switch is determined based on the temperature rate coefficient. It is assumed that the temperature of a semiconductor junction varies from 25°C to 60°C . Fig. 13 shows the failure rate based on different semiconductor junction temperatures according to [25]. Therefore, for the total failure rate, the variation range below is assumed, and it is not a constant in studies.

$$\begin{cases} 3 \leq \lambda \leq 5.9154 \\ 0.9 \leq \lambda_{F-o} \leq 1.77462 \\ 2.1 \leq \lambda_{F-sh} \leq 4.14078 \end{cases} \left(\times 10^{-7} \frac{\text{failure}}{\text{hour}} \right) \quad (28)$$

In this part, the operation of the presented systems over 10000 work hours has been analyzed. Equation (29) shows the equation of the reliability and MTTF.

$$MTTF = \int_0^{\infty} R(t) dt \quad (29)$$

According to the above equation, the reliability and MTTF are directly related to each other. Therefore, by analyzing one of these concepts, most available systems can be specified.

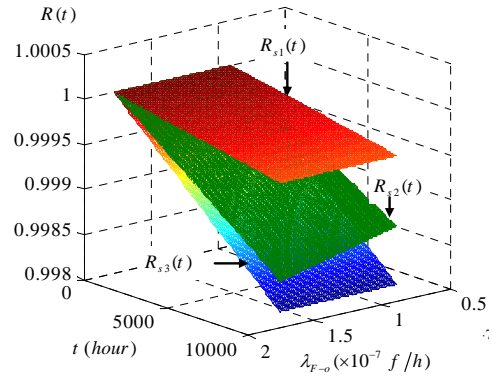


Fig. 14. Comparison of structures 1, 2 and 3 in series configuration.

Because of this, first the reliability of the series configurations are analyzed and compared, and then the parallel configurations are compared. Finally, according to the obtained results, the most reliable or available model in power electronics convertor configurations will be selected.

To prevent confusion, instead of a “redundant structure with similar relays”, a “standby redundant structure with a relay” and a “redundant structure without a relay,” the terms “structures 1, 2 and 3” are used, respectively.

A. Comparison of Series Configurations

In series switch configurations, a SC fault in one switch does not result in a total system failure, and it operates regularly. Therefore, in a series configuration, the importance of an OC fault in these structures, leads to relay implementation. Under these conditions, the SC failure rate is assumed to be constant. Due to variations of the switch failure rate from λ_{N-o} to λ_{F-o} in an OC fault for one of the switches, λ_{F-o} is assumed to be a variable. The variation range according to (28) is described as $0.9 \times 10^{-7} \leq \lambda_{F-o} \leq 1.77462 \times 10^{-7} (f/h)$, and the relaying probability is assumed to be $P_s = 0.9$. In addition, λ_{N-o} and λ_{N-sh} are equal to the minimum values of λ_{F-o} and λ_{F-sh} . They are chosen using (28). λ_{F-sh} is selected as the maximum value of the λ_{F-sh} range.

Fig. 14 shows the reliability variations for the structures 1, 2 and 3 in a series configuration. According to this figure, it is obvious that the reliability of all three structures is equal to $R = 1$ (ideal value) at first. However, it can also be seen that it decreases gradually. This decrement is the maximum for structure 3 and the minimum for structure 1. For a relay-implemented system, it can be deduced that the relay’s proper operation leads to a reliability improvement and a longer lifetime of structures 1 and 2 when compared with structure 3. Therefore, in a series configuration, a redundant structure with a relay under the same conditions has the best reliability and lifetime characteristics.

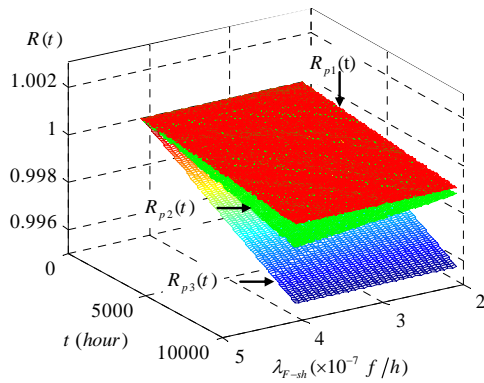


Fig. 15. Comparison of structures 1, 2 and 3 in parallel configuration.

B. Comparison of Parallel Configurations

In parallel configurations, unlike series configurations, the system will not face a total failure under an OC fault condition on one switch. Therefore, it can perform its duty regularly. The importance of a SC fault in this configuration, leads to the implementation of relays. Under these conditions, the OC failure rate is assumed to be constant. Meanwhile, in a SC fault condition for one of the switches, the switch failure rate changes from λ_{N-sh} to λ_{F-sh} . Therefore, λ_{F-sh} is assumed to be variable. The variation range for λ_{F-sh} , according to (28) is described as $2.1 \times 10^{-7} \leq \lambda_{F-sh} \leq 4.14078 \times 10^{-7}$ (f/h), and the relaying probability is assumed to be $P_s = 0.9$. λ_{N-o} and λ_{N-sh} are equal to the minimum values of λ_{F-o} and λ_{F-sh} , and are chosen using (28). λ_{F-o} is selected as the maximum value of the λ_{F-o} range.

Fig. 15 shows the reliability variations for structures 1, 2 and 3 in a parallel configuration. Like the series configuration, the reliability decreases for all of the three structures, and this decrement is the maximum for structure 3 and the minimum for structure 1. In addition, due to the implementation of relays in structures 1 and 2, the reliability of these two structures is better than structure 3. This shows that relays also lead to improved reliability in parallel configurations. Therefore, in parallel configuration, a redundant structure with a relay under the same conditions has the best reliability and lifetime characteristics.

C. Comparison between Series and Parallel Configurations

In this section, an attempt is made to determine the configuration with the greatest reliability. To compare two series and parallel configurations with each other, structures 1 from the two configurations being compared are presented in fig. 16. In this figure, the maximum values for the failure rate are assumed and reliability variations for each of the configurations are shown during 10000 work hours for

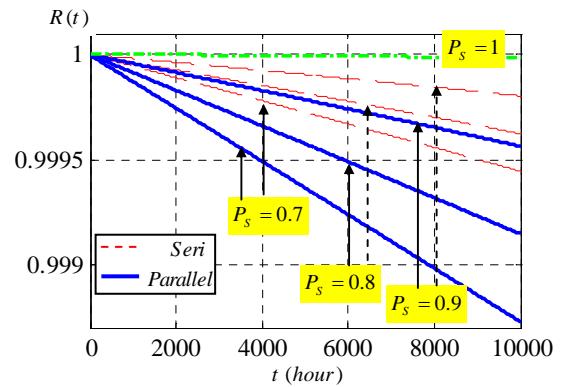


Fig. 16. Comparison of structures 1 in series and parallel configuration with different P_s values.

different P_s . As shown in this figure, four different values for P_s i.e. 0.7, 0.8, 0.9, and 1 are assumed.

The series and parallel configurations are presented with red and blue, respectively. Considering $P_s = 1$, according to (10) and (34), the reliability in a series configuration is equal to that of a parallel configuration. It can be seen in the figure that the two red and blue diagrams have high conformity. For other P_s values, the series configuration is better than the parallel configuration in terms of the reliability and MTTF.

IV. CASE STUDY

The proposed series and parallel structures are applied to conventional boost dc/dc converters. The equivalent circuits of the boost converters with the proposed series and parallel structures are shown in Fig. 17. It is assumed that the switches of the converter turn on at the same time. Simulation results in PSCAD/EMTDC are presented in the following section.

In the series structure, the occurrence of a SC fault in one of the power electronic switches does not impose a problem in terms of the performance of the converter. Meanwhile, an OC fault in one of the switches leads to malfunctioning of the converter. Simulation results of the performance of a converter during a SC fault and an OC fault have been presented in Fig. 18(a) and Fig. 18(b), respectively. In Fig. 18(a), at $t = 2$ s a SC fault occurs on S_1 . However, due to the series structure of the switches, there is no disturbance in the performance of the converter. In Fig. 18(b), the performance of the converter during an OC fault has been analyzed. At $t = 2$ s, S_1 has been confronted with an OC fault that disturbs the correct performance of the converter. Therefore, the reliability of the series structure in facing SC faults of the power electronic switches is higher than that when facing OC faults.

In Fig. 18, v_{s1} and v_{s2} are the voltages across the switches S_1 and S_2 , respectively.

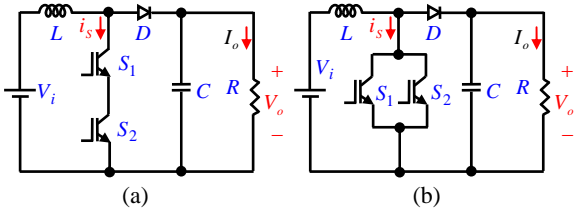


Fig. 17. The equivalent circuit of the boost dc/dc converter, (a) with two series switches, (b) with two parallel switches.

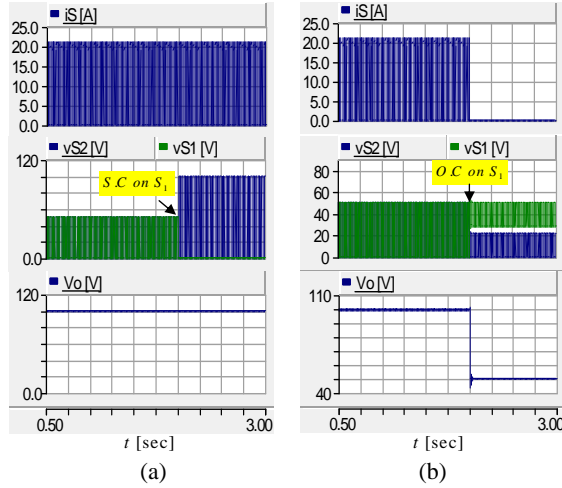


Fig. 18. The voltage and current waveforms of the series structure, (a) during SC fault, (b) during OC fault.

The aforementioned analyzes can also be carried out for the parallel structure. If an SC fault occurs in the circuit depicted in Fig 17(b), there is a disruption in the function of the converter as shown in Fig. 19(a). Meanwhile, despite the occurrence of an OC fault in one of the switches of the parallel structure, the converter can continue its operation as shown in Fig. 19(b).

The problem caused by an OC fault in the series structure can be solved by parallel relays of the switches. The initial states of these relays are open. The equivalent circuit and simulation results of the aforementioned structure have been presented in Fig. 20(a) and Fig. 21(a), respectively. As can be seen in Fig. 21(a), despite the presence of an OC fault in one of the series switches, the converter can perform normally. This is in contrast to Fig. 18(b). Consequently, the presence of relays is necessary for eliminating faults in systems with sensitive loads, which improves the power quality of the load. In addition, in order to increase the reliability in parallel structures during SC faults, series relays with switches can be used. The initial states of these relays are closed. The equivalent circuit and simulation results of the parallel structure with relays have been presented in Fig. 20(b) and Fig. 21(b), respectively. As can be seen from these figures, the results shown in Fig. 21(b) are improved when compared to the ones shown in Fig. 19(b). It must be considered that the duration of the simulation is just for determining the performance of the proposed structure during a fault.

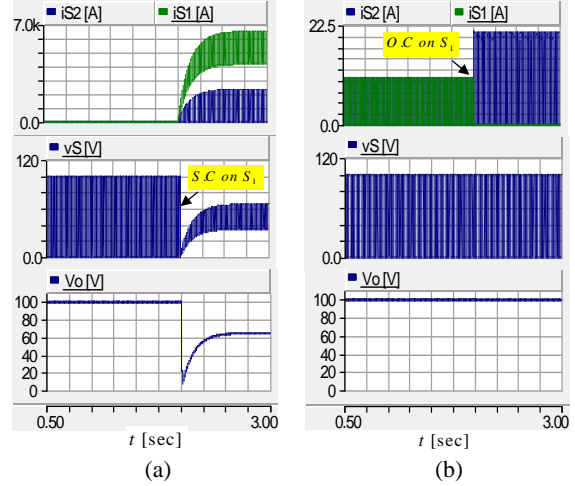


Fig. 19. The voltage and current waveforms of the parallel structure, (a) during SC fault, (b) during OC fault.

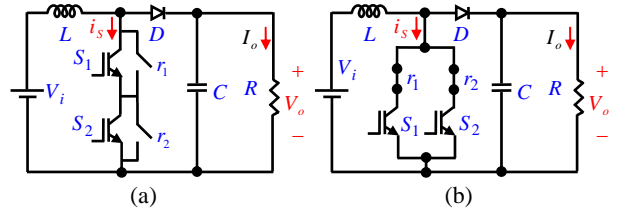


Fig. 20. The equivalent circuit of the boost dc/dc converter with relay, (a) with two series switches, (b) with two parallel switches.

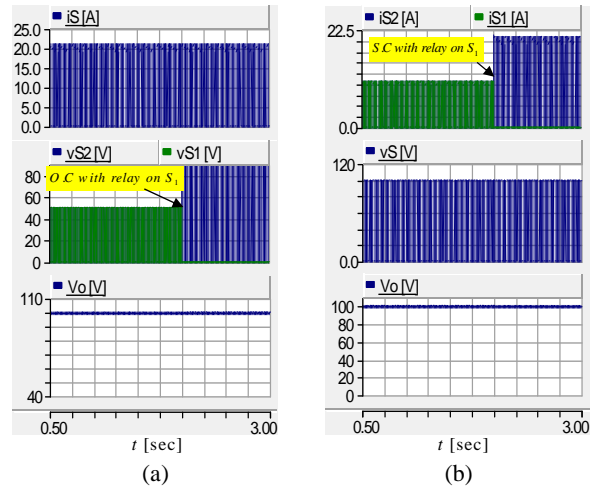


Fig. 21. The voltage and current waveforms of the proposed structure with relays, (a) during OC fault in series structures, (b) during SC fault in parallel structures

In Fig. 19, i_{S1} and i_{S2} are the currents through switches S_1 and S_2 .

If the performances of the diode, inductor, capacitor, and switches lead to better performance of the circuit, they can be considered as series unit elements. Thus, the total reliability of the circuit is equal to the multiplication of each of the elements of the circuit ($R_T(t) = R_{Diode}(t) \times R_{Inductor}(t) \times R_{Capacitor}(t) \times R_{Switch}(t)$). In this paper, the principle idea is increasing reliability based

on the modification of MOSFETs structures while there are no changes applied to the other elements of the circuit. Hence, in this comparison, only the reliability of the switches (the six proposed structures) have been considered, which is representative of the total reliability of each circuit.

V. CONCLUSIONS

In this paper, redundant switches were used in two series and parallel configurations and three structures consisting of a “redundant structure with similar relays,” a “standby redundant structure with a relay” and a “redundant structure without a relay” to improve the MTTF and reliability. The above mentioned structures were also compared. Markov models of each of the mentioned structure have been found. Based on this, their Reliability and MTTF equations are calculated. A comparison indicated that in both the series and parallel configurations, a redundant structure with a relay under the same conditions has the best reliability and MTTF. Comparing the corresponding structures in the series and parallel configurations, the series configuration has a better reliability and MTTF, because the OC failure rate is lower than the SC failure rate.

APPENDIX

The values of a_i ($i = 0$ to 11) in (2) are as follows:

$$\begin{aligned} a_0 &= 1 - [\lambda_{1N-sh} + \lambda_{2N-sh} + P_S \lambda_{1N-o} + P_S \lambda_{2N-o} + (1 - P_S)(\lambda_{1N-o} + \lambda_{2N-o})] \\ a_1 &= \lambda_{1N-sh}, \quad a_2 = \lambda_{2N-sh}, \quad a_3 = P_S \lambda_{1N-o}, \quad a_4 = P_S \lambda_{2N-o} \\ a_5 &= (1 - P_S)(\lambda_{1N-o} + \lambda_{2N-o}), \quad a_6 = 1 - (\lambda_{2F-sh} + \lambda_{2F-o}) \\ a_7 &= \lambda_{2F-sh}, \quad a_8 = \lambda_{2F-o}, \quad a_9 = 1 - (\lambda_{1F-sh} + \lambda_{1F-o}) \\ a_{10} &= \lambda_{1F-sh}, \quad a_{11} = \lambda_{1F-o} \end{aligned}$$

The values of b_i ($i = 0$ to 7) in (11) are as follows:

$$\begin{aligned} b_0 &= 1 - [P_S \lambda_{1F-sh} + P_S^2 \lambda_{1F-o} + (1 - P_S) \lambda_{1F-sh} + (1 - P_S^2) \lambda_{1F-o}] \\ b_1 &= P_S \lambda_{1F-sh}, \quad b_2 = P_S^2 \lambda_{1F-o}, \quad b_3 = (1 - P_S) \lambda_{1N-sh} \\ b_4 &= 1 - (\lambda_{2F-sh} + \lambda_{2F-o}), \quad b_5 = \lambda_{2F-sh}, \quad b_6 = \lambda_{2F-o}, \quad b_7 = (1 - P_S^2) \lambda_{1F-o} \end{aligned}$$

The values of c_i ($i = 0$ to 9) in (14) are as follows:

$$\begin{aligned} c_0 &= 1 - (\lambda_{1N-sh} + \lambda_{2N-sh} + \lambda_{1N-o} + \lambda_{2N-o}) \\ c_1 &= \lambda_{1N-sh}, \quad c_2 = \lambda_{2N-sh}, \quad c_3 = \lambda_{1N-o} + \lambda_{2N-o} \\ c_4 &= 1 - (\lambda_{2F-sh} + \lambda_{2F-o}), \quad c_5 = \lambda_{2F-sh}, \quad c_6 = \lambda_{2F-o} \\ c_7 &= 1 - (\lambda_{1F-sh} + \lambda_{1F-o}), \quad c_8 = \lambda_{1F-sh}, \quad c_9 = \lambda_{1F-o} \end{aligned}$$

The values of d_i ($i = 0$ to 11) in (17) are as follows:

$$\begin{aligned} d_0 &= 1 - [P_S \lambda_{1N-sh} + P_S \lambda_{2N-sh} + (1 - P_S)(\lambda_{1N-sh} + \lambda_{2N-sh}) + \lambda_{1N-o} + \lambda_{2N-o}] \\ d_1 &= P_S \lambda_{1N-sh}, \quad d_2 = P_S \lambda_{2N-sh}, \quad d_3 = (1 - P_S)(\lambda_{1N-sh} + \lambda_{2N-sh}) \\ d_4 &= \lambda_{2N-o}, \quad d_5 = \lambda_{1N-o}, \quad d_6 = 1 - (\lambda_{2F-sh} + \lambda_{2F-o}) \\ d_7 &= \lambda_{2F-sh}, \quad d_8 = \lambda_{2F-o}, \quad d_9 = 1 - (\lambda_{1F-sh} + \lambda_{1F-o}) \\ d_{10} &= \lambda_{1F-sh}, \quad d_{11} = \lambda_{1F-o} \end{aligned}$$

The values of g_i ($i = 0$ to 7) in (20) are as follows:

$$\begin{aligned} g_0 &= 1 - [P_S^2 \lambda_{1F-sh} + P_S \lambda_{1F-o} + (1 - P_S^2) \lambda_{1F-sh} + (1 - P_S) \lambda_{1F-o}] \\ g_1 &= P_S^2 \lambda_{1F-sh}, \quad g_2 = P_S \lambda_{1F-o} \\ g_3 &= (1 - P_S^2) \lambda_{1N-sh}, \quad g_4 = (1 - P_S) \lambda_{1F-o} \\ g_5 &= 1 - (\lambda_{2F-sh} + \lambda_{2F-o}), \quad g_6 = \lambda_{2F-sh}, \quad g_7 = \lambda_{2F-o} \end{aligned}$$

The values of h_i ($i = 0$ to 9) in (23) are as follows:

$$\begin{aligned} h_0 &= 1 - (\lambda_{1N-sh} + \lambda_{2N-sh} + \lambda_{1N-o} + \lambda_{2N-o}) \\ h_1 &= \lambda_{1N-o}, \quad h_2 = \lambda_{2N-o}, \quad h_3 = \lambda_{1N-sh} + \lambda_{2N-sh} \\ h_4 &= 1 - (\lambda_{2F-sh} + \lambda_{2F-o}), \quad h_5 = \lambda_{2F-sh}, \quad h_6 = \lambda_{2F-o} \\ h_7 &= 1 - (\lambda_{1F-sh} + \lambda_{1F-o}), \quad h_8 = \lambda_{1F-sh}, \quad h_9 = \lambda_{1F-o} \end{aligned}$$

REFERENCES

- [1] L. R. Gopi Reddy, L. M. Tolbert, and B. Ozpineci, “Power cycle testing of power switches: a literature survey,” *IEEE Trans. Power Electron.*, Vol. 30, No. 5, pp. 2465-2473, 2015.
- [2] Y. Song and B. Wang, “Survey on reliability of power electronic systems,” *IEEE Trans. Power Electron.*, Vol. 28, No. 1, pp. 591-604, Apr. 2012.
- [3] U. M. Choi, F. Blaabjerg, and K. B. Lee, “Reliability improvement of a T-type three-level inverter with fault-tolerant control strategy,” *IEEE Trans. Power Electron.*, Vol. 30, No. 5, pp. 2660-2673, May 2015.
- [4] A. Tajfar and S. K. Mazumder, “A fault-tolerant switching scheme for an isolated DC/AC matrix converter,” *IEEE Trans. Power Electron.*, Vol. 30, No. 5, pp. 2798-2813, May 2015.
- [5] A. Alghassi, S. Perinpanayagam, M. Samie, and T. Sreenuch, “Computationally efficient, real-time, and embeddable prognostic techniques for power electronics,” *IEEE Trans. Power Electron.*, Vol. 30, No. 5, pp. 2623-2634, May 2015.
- [6] Y. Chen, Y. Nan, Q. Kong, and S. Zhong, “An input-adaptive self-oscillating boost converter for fault-tolerant LED driving with wide-range ultralow voltage input,” *IEEE Trans. Power Electron.*, Vol. 30, No. 5, pp. 2743-2752, May 2015.
- [7] X. Sun, Y. Zhou, W. Wang, B. Wang, and Z. Zhang, “Alternative source-port-tolerant series-connected double-input DC-DC converter,” *IEEE Trans. Power Electron.*, Vol. 30, No. 5, pp. 2733-2742, May 2015.
- [8] C. Petit, A. Meinertzhagen, D. Zander, O. Simonetti, M. Fadlallah, and T. Maurel, “Low voltage SILC and P- and N-MOSFET gate oxide reliability,” *Microelectronics Reliability*, Vol. 45, No. 3-4, pp. 479-485, Mar./Apr. 2005.
- [9] H. Kaur, S. Kabra, S. Bindra, S. Haldar, and R. S. Gupta, “Impact of graded channel (GC) design in fully depleted cylindrical/surrounding gate MOSFET (FD CGT/SGT) for improved short channel immunity and hot carrier reliability,” *Solid-State Electronics*, Vol. 51, No. 3, pp. 398-404, Mar. 2007.
- [10] R. Fernández, R. Rodríguez, M. Nafría, X. Aymerich, B. Kaczer, and G. Groeseneken, “FinFET and MOSFET preliminary comparison of gate oxide reliability,” *Elsevier Microelectronics Reliability*, Vol. 46, No. 9-11, pp. 1608-1611, Sep./Nov. 2006.
- [11] C. Busca, R. Teodorescu, F. Blaabjerg, S. Munk-Nielsen,

- L. Helle, T. Abeyasekera, and P. Rodriguez, "An overview of the reliability prediction related aspects of high power IGBTs in wind power applications," *Elsevier Microelectronics Reliability*, Vol. 51, No. 9-11, pp. 1903-1907, Sep./Nov. 2011.
- [12] E. E. Kostanyan and K. Ma, "Reliability estimation with uncertainties consideration for high power IGBTs in 2.3 MW wind turbine converter system," *Elsevier Microelectronics Reliability*, Vol. 52, No. 9-10, pp. 2403-2408, Sep./Oct. 2012.
- [13] Y. Song and B. Wang, "Survey on reliability of power electronic systems," *IEEE Trans. Power Electron.*, Vol. 28, No. 1, pp. 591-604, Jan. 2013.
- [14] H. Wang and F. Blaabjerg, "Reliability of capacitors for DC-Link applications in power electronic converters – An overview," *IEEE Trans. Ind. Appl.*, Vol. 50, No. 5, pp. 3569-3578, Sep. 2014.
- [15] W. Zhang, D. Xu, P. N. Enjeti, H. Li, J. T. Hawke, and H. S. Krishnamoorthy, "Survey on fault-tolerant techniques for power electronic converters," *IEEE Trans. Power Electron.*, Vol. 29, No. 12, pp. 6319-6331, Dec. 2014.
- [16] B. Mirafzal, "Survey of fault-tolerance techniques for three-phase voltage source inverters," *IEEE Trans. Ind. Electron.*, Vol. 61, No. 10, pp. 5192-5202, Oct. 2014.
- [17] J.-C. Lee, T.-J. Kim, D.-W. Kang, and D.-S. Hyun, "A control method for improvement of reliability in fault tolerant NPC inverter system," in *Proc. IEEE Power Electron. Specialists Conf.*, pp. 1-5, 2006.
- [18] F. Richardeau and T. T. L. Pham, "Reliability calculation of multilevel converters: Theory and applications," *IEEE Trans. Ind. Electron.*, Vol. 60, No. 10, pp. 4225-4233, Oct. 2013.
- [19] M. Arifujjaman, "Reliability comparison of power electronic converters for grid-connected 1.5kW wind energy conversion system," *Renewable Energy*, Vol. 57, pp. 348-357, Sep. 2013.
- [20] X. Yu and A. M. Khambadkone, "Reliability analysis and cost optimization of parallel-inverter system," *IEEE Trans. Ind. Electron.*, Vol. 59, No. 10, pp. 3881-3889, Oct. 2012.
- [21] E. G. Strangas, S. Aviyente, J. D. Neely, and S. S. H. Zaidi, "The effect of failure prognosis and mitigation on the reliability of permanent-magnet AC motor drives," *IEEE Trans. Ind. Electron.*, Vol. 60, No. 8, pp. 3519-3528, Aug. 2013.
- [22] V. Esteve, J. Jordán, E. S. Kilders, E. J. Dede, E. Maset, J. B. Ejea, and A. Ferreres, "Improving the reliability of series resonant inverters for induction heating applications," *IEEE Trans. Ind. Electron.*, Vol. 61, No. 5, pp. 2564-2572, May 2014.
- [23] A.E. Khosroshahi, M. Abapour, and M. sabahi, "Reliability evaluation of conventional and interleaved DC-DC boost converters," *IEEE Trans. Power Electron.* Vol. 30, No. 10, pp. 5821-5828, Oct. 2015.
- [24] D. J. Smith, *Reliability, Maintainability and Risk 8th Edition: Practical Methods for Engineers including Reliability Centred Maintenance and Safety-Related Systems*, Elsevier, Great Britain, Appendix 5: Failure Mode Percentages, 2011.
- [25] *Reliability prediction of electronic equipments*, Relex Software Corp., Greensburg, PA, Rep. MIL-HDBK-217, 1990.



Mohsen Hasan Babayi Nozadian was born in Urmia, Iran, in January 1991. He received his B.S. degree (graduating at the top of his class) in Power Electrical Engineering from the Faculty of Engineering, University of Urmia, Urmia, Iran, in 2013; and his M.S. degree in Power Electronics from the Department of Electrical and Computer Engineering, University of Tabriz, Tabriz, Iran, in 2015. He has been working towards his Ph.D. degree in the Department of Electrical and Computer Engineering, University of Tabriz, since September 2015. His current research interests include the improvement and design of power electronic converters, Z-source converters, and the reliability of power electronics converters.



University of Tabriz, Tabriz, Iran, in 2015.

Mohammad Shadnam Zarbil was born in Kaleybar, East Azerbaijan, Iran, in 1990. He received his B.S. degrees (with first class Honors) in Electrical Power Engineering from the University of Azarbaijan Shahid Madani, Tabriz, Iran, in 2013; and his M.S. degree in Electrical Power Engineering (Power Electronics and Systems) from the University of Tabriz, Tabriz, Iran, in 2015.



University of Tabriz, Tabriz, Iran, in 2005 and 2007, respectively; and his Ph.D. degree in Electrical Engineering from the Tarbiat Modares University, Tehran, Iran, in 2013. He is presently working as an Assistant Professor in the School of Electrical and Computer Engineering, University of Tabriz. His current research interests include reliability, energy management, power system protection and transients.

Mehdi Abapour (M'12) received his B.S. and M.S. degrees in Electrical Engineering from the University of Tabriz, Tabriz, Iran, in 2005 and 2007, respectively; and his Ph.D. degree in Electrical Engineering from the Tarbiat Modares University, Tehran, Iran, in 2013. He is presently working as an Assistant Professor in the School of Electrical and Computer Engineering, University of Tabriz. His current research interests include reliability, energy management, power system protection and transients.